Enhanced function of pancreatic islets co-encapsulated with ECM proteins and mesenchymal stromal cells in a silk hydrogel

Nicolynn E. Davis [a], Liese N. Beenken-Rothkopf [b], Annie Mirsoian [a], Nikola Kojic [c], David L. Kaplan [c], Annelise E. Barron [b], Magali J. Fontaine [a],*

[a] Department of Pathology, Stanford University School of Medicine, 300 Pasteur Drive, H1402, M/C 5626, Stanford, CA 94305-5626, USA
[b] Department of Bioengineering, Stanford School of Medicine, Stanford, CA 94305, USA
[c] Department of Biomedical Engineering, Tufts University, Medford, MA 02155, USA

ARTICLE INFO

ABSTRACT

Pancreatic islet encapsulation within biosynthetic materials has had limited clinical success due to loss of islet function and cell death. As an alternative encapsulation material, a silk-based scaffold was developed to reestablish the islet microenvironment lost during cell isolation. Islets were encapsulated with ECM proteins (laminin and collagen IV) and mesenchymal stromal cells (MSCs), known to have immunomodulatory properties or to enhance islet cell graft survival and function. After a 7 day in vitro encapsulation, islets remained viable and maintained insulin secretion in response to glucose stimulation. Islets encapsulated with collagen IV, or laminin had increased insulin secretion at day 2 and day 7, respectively. A 3.2-fold synergistic improvement in islet insulin secretion was observed when islets were co-encapsulated with MSCs and ECM proteins. Furthermore, encapsulated islets had increased gene expression of functional genes; insulin I, insulin II, glucagon, somatostatin, and PDX-1, and lower expression of the de-differentiation genes cytokeratin 19 and vimentin compared to non-encapsulated cells. This work demonstrates that encapsulation in silk with both MSCs and ECM proteins enhances islet function and with further development may have potential as a suitable platform for islet delivery in vivo.

© 2012 Elsevier Ltd. All rights reserved.

1. Introduction

Type 1 diabetes (T1D) is characterized as an autoimmune-mediated destruction of insulin-producing β-cells within pancreatic islets, leading to insufficient regulation of blood glucose levels. Islet cell transplantation offers therapeutic potential for patients with T1D to normalize glucose metabolism and prevent the complications of the disease [1]. Despite many advances, transplantation success rates have been limited by islet cell death in the early post-transplant period, followed by a long-term decline in islet function and viability [2]. Significant challenges to islet transplantation remain, including preservation of islet cells during isolation, revascularization of islets after implantation, and prevention of inflammation and autoimmune destruction of the islet graft. An emerging therapeutic strategy involves the use of biomaterials to encapsulate islets and overcome these obstacles. Biomaterials may enhance islet function by providing a three-dimensional cellular support and delivering proteins, growth factors, and immunosuppressive agents [3,4].

Current natural and synthetic materials for islet encapsulation have had limited success due to fibroblast overgrowth and mechanical or chemical instability. Some polymeric systems have shown reduced viability and functionality of the islet cells due to polymer biodegradation and limited permeability of the capsules [5]. Consequently, alternative encapsulation materials are needed for islet transplantation. In this study, a hydrogel based on self-assembling silk fibroin proteins from the Bombyx mori silkworm was investigated for islet encapsulation. Silk fibroin supports cell adhesion, proliferation and differentiation, and has good material properties such as biocompatibility, slow degradation rate, and strong mechanical integrity [6]. Although silk-based hydrogels have been investigated for encapsulation of a variety of cell types, they have not been used for islet encapsulation or transplantation. In the present study, silk was used to recreate the islet microenvironment necessary for long-term islet graft function.

Natural stimuli from the islet microenvironment arise from contact with ECM proteins and trophic factors secreted by the surrounding cells that promote islet survival and proliferation to maintain β-cell mass. In synthetic hydrogels, ECM proteins have been co-encapsulated with islets to restore the native microenvironment damaged during cell isolation as a way to enhance islet graft function and survival [7–10]. Moreover co-encapsulation of islets with stromal cells may replenish the nutrients and growth factors critical for islet graft maintenance. Previously, mesenchymal stromal cells (MSCs) were shown to secrete regulatory islet growth factors that are angiogenic, anti-apoptotic, and proliferation-stimulating (i.e.: HGF, TGF-β1 and IL-6) [11–13]. Additionally, MSCs have immunomodulatory properties that reduce inflammatory cytokine production and suppress allo-immune responses [14,15]. For these reasons, the co-encapsulation and transplantation of MSCs with islets can improve allograft survival and function [14,15].

Although the co-transplantation of islets with MSCs has been gaining traction, to date, there has not been a hydrogel platform that has co-encapsulated MSCs and islets with ECM proteins as a means to enhance graft survival. In the present study, silk hydrogels are investigated in vitro as an islet encapsulation platform to co-encapsulate islets, ECM proteins and MSCs to maintain or enhance islet function.

2. Methods

2.1. Silk hydrogel formation and incorporation of ECM proteins

Silk fibroin solutions were supplied by Kaplan et al. and prepared as previously described [16]. Silk self-assembly and gelation was vortex-induced by mixing 375 μL of 8 wt% silk fibroin with 625 μL of sterile water in a glass vial and vortexing for 7 min at 3200 rpm (VWR International, Radnor, PA). After phase separation, the white solid-like material was removed and the remaining silk solution was diluted 2-fold with media and allowed to gel for 2 h at 37 °C. For some experiments, silk hydrogels were formed with two different ECM components, collagen type IV (Sigma, St. Louis, MO), and laminin (BD Biosciences, San Jose, CA) which were added to the silk solution after vortexing to achieve a final concentration of 100 μg/mL of silk hydrogel solution (0.7 wt% ECM protein each by mass of total hydrogel dry weight).

To determine if ECM proteins were evenly distributed throughout the gel, 15 μL silk hydrogels with laminin were formed directly onto an 8-chamber cover glass slide (Nalge International, Rochester, NY), washed 3 times with 200 μL DPBS (Mediatech, Inc. Manassas, VA) and stained in three steps: 1) blocked with 10% fetal bovine serum (FBS) (Gemini Bio-Products, West Sacramento, CA); 2) incubated with a rabbit polyclonal laminin antibody (1:200) (Abcam Inc., Cambridge, MA); and 3) incubated with an Alexa Fluor 488 goat anti-rabbit IgG secondary antibody (1:200) (Invitrogen, Carlsbad, CA), each for 1 h, and separated with 3 DPBS washes for 5 min each. Silk hydrogels with laminin incubated only with secondary antibody served as controls. Positive samples fluoresced green with excitation and emission wavelengths of ∼495 nm and ∼635 nm, respectively.

2.2. Silk rheology

Silk hydrogel bulk material properties were determined by oscillatory rheology. Rheological experiments were performed with an Anton-Paar Physica MCR Rheometer (Ashland, VA) with a stainless steel cone and plate (25 mm diameter, 1° angle) and peltier temperature control. After the silk was vortexed (as described above) and mixed 1:1 with cRPMI media (10% FBS, 1% pen/strep), 160 μL of the final solution was added to the rheometer. A humid chamber was created around the sample by placing a layer of wet Kimwipes around the platform and placing the thermostat chamber on top. For frequency and strain sweep experiments, the measuring device was lowered to the measuring height and held for 2 h at 37 °C. Storage and loss modulus measurements during frequency sweeps were completed in the oscillator mode at 1% strain, and strain sweep experiments were performed with a strain ranging from 0.1% to 100% at an angular frequency of 10 s^{-1}.

2.3. Animals

Fourteen-week-old BALB/c or C57Bl/6 female mice were obtained from Jackson Laboratory (Bar Harbor, ME). All animals were housed in the Stanford Blood Center animal facility and used in compliance with the Institutional Animal Care and Use Committee (IACUC). Animal manipulations were conducted using protocols approved by the IACUC. All animals were sacrificed on the day of organ harvest and islet or splenocyte isolation.

2.4. Islet isolation and culture

The islet isolation procedure was modified from Li et al. [17], BALB/c animals were anesthetized and the abdomen opened. The pancreas was injected through the main bile duct with collagenase type V (Sigma, St Louis, MO) at 0.7 mg/mL in a perfusion solution (Cellgro-Mediatech, Inc, Herndon, VA). The distended pancreas was surgically removed and digested in a 37 °C water bath for 15 min with vigorous agitation. Free islets, released from the digested pancreatic tissue were purified by centrifugation on Euro-Ficoll gradients (Mediatech, Herndon, VA), handpicked, counted, and cultured with cRPMI (10% FBS and 1% pen/strep) overnight in a humidified incubator at 37 °C with 5% CO$_2$.

2.5. MSC culture and characterization

Bone marrow derived MSCs from C57Bl/6 mice were provided by the Texas A&M Health Science Center College of Medicine Institute for Regenerative Medicine at Scott & White. MSCs were cultured according to supplier's recommendations in MSC media; DMEM with 10% MSC-qualified FBS (Invitrogen, Carlsbad, California), 10% Horse serum (Thermo Fisher Scientific, Waltham, MA), 1% Antibiotic/Antimycotic (Invitrogen), and 1% L-glutamine (Sigma). MSCs were characterized by the supplier before material transfer and after culturing in our facility for ability to differentiate and for surface marker phenotype expression. The ability of MSCs to differentiate into bone was verified by Alizarin red staining of mineral deposits and microscopy following reported methods [18].

MSC phenotype was characterized with multicolor flow cytometry by immunostaining with fluorochrome-conjugated mAbs for the appropriate isotype controls or against the following surface antigens: CD11b Pacific Blue, CD29 APC/Cy7, CD34 APC, CD45 PerCP/Cy5.5, and CD106 PE/Cy7 (Biolegend, San Diego, CA); CD31 PE, and Sca-1 FITC (BD Pharmingen, San Diego, CA). MSCs at passage 20 were trypsinized with 0.25% Trypsin with EDTA (Invitrogen) for 2 min, washed with FACS buffer (0.1% BSA in PBS), and enumerated via trypan blue exclusion. Approximately 1×10^6 cells per sample were incubated in FcR block (Biolegend) for 5 min at 4 °C before adding the fluorochrome-conjugated mAbs per manufacturers' recommendations. DAPI, a viability dye was added 2 min prior to washing the cells in FACS buffer. Following centrifugation, the cell pellets were resuspended in FACS buffer and data acquired using the LSRII instrument (BD Biosciences,San Jose, CA). The files were analyzed via FlowJo software (Tree Star, Inc, Ashland, OR).

2.5.1. MSC suppression of splenocyte proliferation

MSC suppression of immune activation was assessed by mixed lymphocyte reactions. Splenocytes were isolated from both BALB/c (stimulators) and C57Bl/6 (responders) mice. Silk encapsulated MSCs were cultured at 2×10^5 cells/well in 30 μL of silk hydrogel and placed in the inner chamber of a transwell membrane (0.2 μm pore size) (Millipore) in a 96-well round bottom plate. Splenocytes were cultured in the bottom well at 2×10^5 cells/well with either 2×10^5 irradiated (30 Gy) stimulator allo-splenocytes or with Dynabeads Mouse T-activator C3/CD28 beads (Invitrogen) at a bead-to-cell ratio of 1:10. After 72 h, the splenocytes were pulsed with 3H-thymidine (3H-TdR) for 16 h. Thymidine incorporation was measured with a liquid scintillation counter (Perkin Elmer Wallac 1450 Microbeta Plus, Waltham, MA) and results expressed as mean counts per minute (cpm), $n \geq 5$.

2.6. Cell encapsulation in the hydrogels

Islets were encapsulated in silk hydrogels ∼24 h after isolation. Handpicked islets were suspended in 100 μL cRPMI, pelleted at 3000 g for 5 min, and resuspended in 20 μL of silk solution that had been vortexed and diluted with cRPMI with or without ECM proteins as described above. The hydrogel suspension was incubated for 2 h at 37 °C for gelation before the addition of cRPMI media. For islet co-encapsulation with MSCs, MSCs were counted and added at 1000 MSCs per islet cell to the vortexed silk solution before resuspension with islets.

2.7. Islet viability and glucose stimulated insulin secretion

The viability of islets encapsulated in silk hydrogels with ECM components was assessed using fluorescence staining for cell membrane integrity and intracellular esterase activity. Islets in silk hydrogels were imaged on a glass insert in a 35 mm glass bottom microwell dish (MatTek Corporation, Ashland, MA). Islet viability was assessed after a 7 day silk hydrogel encapsulation, by staining with 1 mL of 2 μM calcein AM and 3 μM ethidium homodimer-1 from the LIVE/DEAD viability assay kit (Invitrogen, Eugene, OR) in phosphate buffer saline (PBS) for 30 min at 37 °C. Viable cells with intact membranes fluoresced green by the reaction of calcein AM with intracellular esterases, and non-viable cells were stained red by the intracellular diffusion of ethidium homodimer-1 into cells with damaged membranes. Images were acquired using laser scanning confocal microscopy on a Zeiss LSM 510 META microscope (Zeiss, Germany) at the Stanford University Cell Science Imaging Facility (CSIF) (Stanford, CA). Samples with 15 islets each (approximately 11 IEQs) ($n = 3$) were analyzed with multiple images of individual islets in the z-axis and stacked using ImageJ software (NIH, rsb.info.nih.gov/ij/).

Islet function was assessed *in vitro* by a glucose challenge. Islets encapsulated in silk hydrogels (20 islets each, approximately 15 IEQs) were cultured on a tissue culture insert (12 μm pore size) (Millipore, Billerica, MA) in a 24-well plate. Samples were washed for 5 min with 2.5 mM glucose in Krebs−Ringer buffer (0.1% BSA, 25 mM HEPES, 115 mM NaCl, 24 mM NAHCO₃, 5 mM KCl, 1 mM MgCl₂, 2.5 mM CaCl₂). Following the wash, samples underwent a static incubation for 60 min each, with low (2.5 mM) followed by high (16.7 mM) glucose concentrations in Krebs−Ringer buffer. Insulin secretion was measured using a mouse insulin enzyme-linked immunosorbent assay (ELISA) kit (Mercodia, Winston-Salem, NC). Values are reported as a stimulation index (SI) (ratio of insulin secreted with high glucose (μg/L) over insulin secreted with low glucose stimulation (μg/L)). For all conditions $n \geq 5$.

2.8. Islet RNA extraction and qRT-PCR

Analysis of mRNA levels of islet functional genes (insulin I, insulin II, glucagon, somatostatin, PDX-1) and de-differentiation genes (cytokeratin 19, vimentin, E-cadherin) were assessed with real time qRT-PCR. Total islet RNA was extracted by thoroughly pipetting the hydrogel to disrupt the gel network and using the RNeasy Plus Mini Kit (Qiagen, Valencia, CA) with RNase-Free DNase Set (Qiagen) according to the manufacturer's recommendations for on-column treatment. Purified RNA concentration and quality was measured by the NanoDrop1000 Spectrophotometer (Thermo Scientific), and reverse transcription was carried out using the High Capacity cDNA Reverse Transcription Kit (Applied Biosystems, Carlsbad, CA). To increase starting material, approximately 20 ng of cDNA was used for pre-amplification with TaqMan PreAmp Master Mix (Applied Biosystems). Gene expression was analyzed with 20 μL total volume using the ABI 7500 FAST machine (ABI, Foster City, CA) with probes from the TaqMan Gene Expression Assays with TaqMan Gene Expression Master Mix (Applied Biosystems). All assays were carried out in duplicate in 96-well format plates. For an internal control, both GAPDH and beta-actin expression remained stable in all conditions studied. The 2ΔΔCT method [19] was used to calculate the relative gene expression using GAPDH for normalization. Changes in the target gene expression of islets encapsulated in silk with ECM proteins were expressed as fold-change from the value of non-encapsulated islets. For all conditions $n \geq 4$.

2.9. Statistical analysis

All statistics were performed using GraphPad Prism 5 (La Jolla, CA) with a two-sample *T* test assuming unequal variances. *p*-values less than 0.05 were considered significant.

3. Results

3.1. Incorporation of ECM proteins in silk hydrogels

Silk hydrogels were formed in the presence of two ECM proteins (collagen IV and laminin) to investigate the influence of ECM signaling on encapsulated islet cell survival and function. ECM proteins were encapsulated at 100 μg/mL of gel, based on concentrations tested in previous studies [8]. Immunostaining using a primary polyclonal laminin-specific antibody and a secondary Alexa Fluor 488 fluorescent antibody showed uniform laminin distribution throughout the hydrogel (data not shown). The distribution of collagen IV in the silk hydrogel was assumed to be comparable to laminin as previously reported [8].

The material properties of the silk hydrogel were measured by oscillatory rheometry. As previously reported, Yucel et al. demonstrated that vortexing low-viscosity silk solutions induced formation of hydrogels with permanent, physical, intermolecular crosslinks and varying material properties [16]. At the concentration used in this study (1.5 wt% silk), the material storage modulus was ∼ 1 kPa (data not shown). The addition of ECM proteins did not significantly affect the hydrogel storage modulus as determined by both a strain and frequency sweep (data not shown).

3.2. Islet encapsulation in silk hydrogels with ECM proteins

Islets encapsulated in silk hydrogels with or without ECM proteins maintained their round morphology and three-dimensional capsule up to 7 days post-encapsulation (Fig. 1A). At 7 days, the relative quantity of viable cells per islet was assessed using LIVE/DEAD fluorescent staining and microscopy (Fig. 1B). Islets
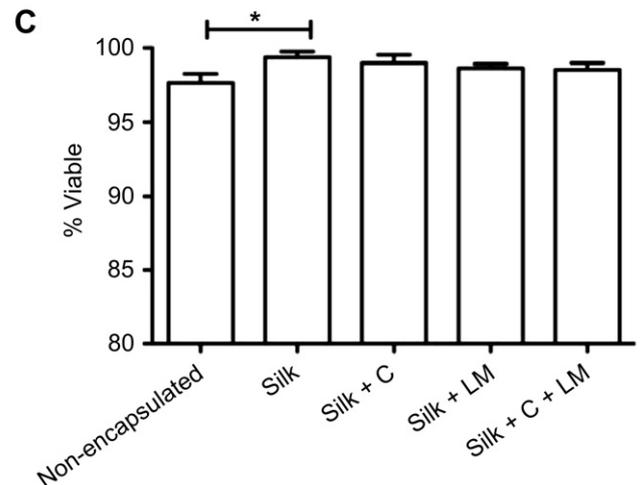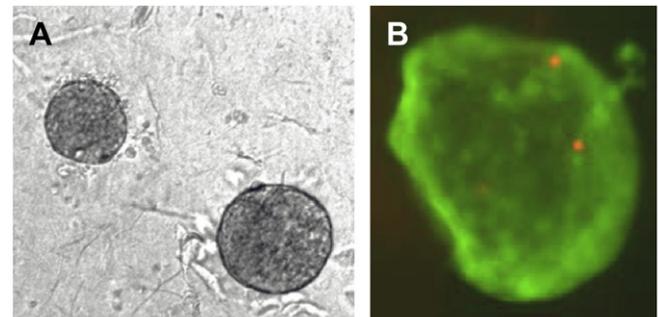
Fig. 1. Islet viability after 7 days of encapsulation in silk hydrogels with ECM proteins collagen IV (C) and laminin (LM). (A) Brightfield image of islets encapsulated in a silk hydrogel after 7 days (10 × magnification). (B) Fluorescent stacked image of islets stained with LIVE/DEAD viability stain after 7 days (10 × magnification). Viable cells fluoresce green and apoptotic cells fluoresce red. (C) Quantitative analysis of islet viability after a 7 day encapsulation in silk, mean ± SEM, for all conditions $n \geq 12$. *$p < 0.05$, compared to non-encapsulated islets.

encapsulated in silk had greater than 98% cell viability, which was significantly higher than non-encapsulated islets (Fig. 1C) ($p < 0.05$).

3.3. Encapsulated islet response to glucose stimulation

Islet insulin secretion in response to glucose stimulation was assessed after a 2 day and 7 day silk hydrogel encapsulation (Fig. 2). After 2 days, islets encapsulated in silk with and without ECM proteins had an SI greater than 1.0, and islets encapsulated with ECM proteins performed better than both non-encapsulated islets and islets encapsulated without ECM proteins (Fig. 2A). Islets in silk with collagen IV showed a significant improvement in SI compared to non-encapsulated islets (1.6 vs 1.2, $p < 0.05$). However, the SI for islets in silk without ECM proteins was lower than for non-encapsulated cells ($p < 0.05$). After 7 days, silk encapsulated islets with laminin showed the greatest SI at 2.0, compared to non-encapsulated islets with an SI of 1.2 ($p < 0.01$) (Fig. 2B). At both time points, the SI for islets encapsulated in silk with both collagen and laminin was lower or equivalent to SI for islets in silk with either collagen or laminin alone.

3.4. Islet gene expression with ECM proteins

After a 7 day encapsulation, expression of functional genes (insulin I, insulin II, glucagon, and somatostatin) and the pancreatic
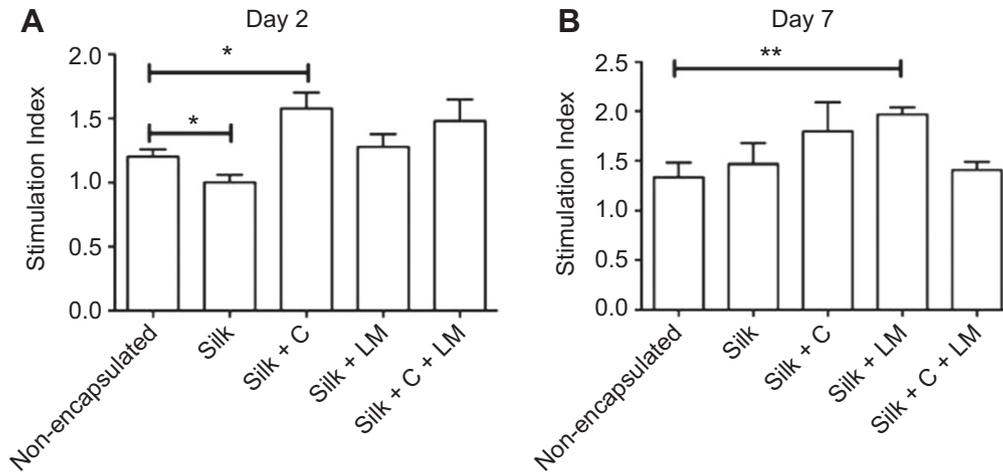
Fig. 2. Islet response to glucose stimulation in hydrogels with ECM proteins collagen IV (C) and laminin (LM). Insulin secretion is given as the stimulation index, which is the ratio of insulin secreted in response to 16.7 mM glucose to insulin secreted in response to 2.5 mM glucose, after 2 days (A) or 7 days (B) of encapsulation, mean ± SEM, for all conditions $n \geq 4$. $^*p < 0.05$, $^{**}p < 0.01$, compared to non-encapsulated islets.

and duodenal homeobox 1 (PDX-1) transcription factor were increased for all formulations of islets encapsulated in silk compared to non-encapsulated islets (Fig. 3A). Islets in silk with both ECM proteins had significantly higher expression of both insulin genes than did islets in silk without ECM proteins ($p < 0.05$). There was no significant change in glucagon and somatostatin gene expression with the presence of ECM proteins. PDX-1 expression was increased 5.6-fold for islets in silk with collagen IV, 5.3-fold for islets in silk with both collagen IV and laminin, and 3.9-fold for islets in silk without ECM proteins, as compared to non-encapsulated islets ($p < 0.05$).

Changes in islet expression of de-differentiation genes E-cadherin (Ecad), cytokeratin 19 (Krt19), and vimentin (Vim) were analyzed by qRT-PCR after a 7 day encapsulation in silk (Fig. 3B). Ecad expression was increased between 1.5 and 2.2-fold for all formulations of islets in silk compared to non-encapsulated islets.

Furthermore, islets in silk with laminin had a significantly lower change in Ecad expression than did islets in silk without ECM proteins ($p < 0.05$). For all formulations of islets in silk, both the Krt19 and Vim had lower gene expression levels than non-encapsulated islets, ranging between 0.5 and 0.8-fold.

3.5. MSC phenotype characterization and function in silk

The phenotype of the mouse bone marrow-derived MSCs was characterized by flow cytometry in our laboratory at passage 20. MSCs were positive for CD29, Sca-1, CD106, and CD34; and negative for CD11b, CD31, and CD45 (markers for macrophages, endothelial, and hematopoietic cells) (data not shown), consistent with the supplier's characterization at passage 7–8. Furthermore, MSCs were able to differentiate *in vitro* into osteoblast-like cells, as assessed by staining with Alizarin Red (data not shown). In a mixed
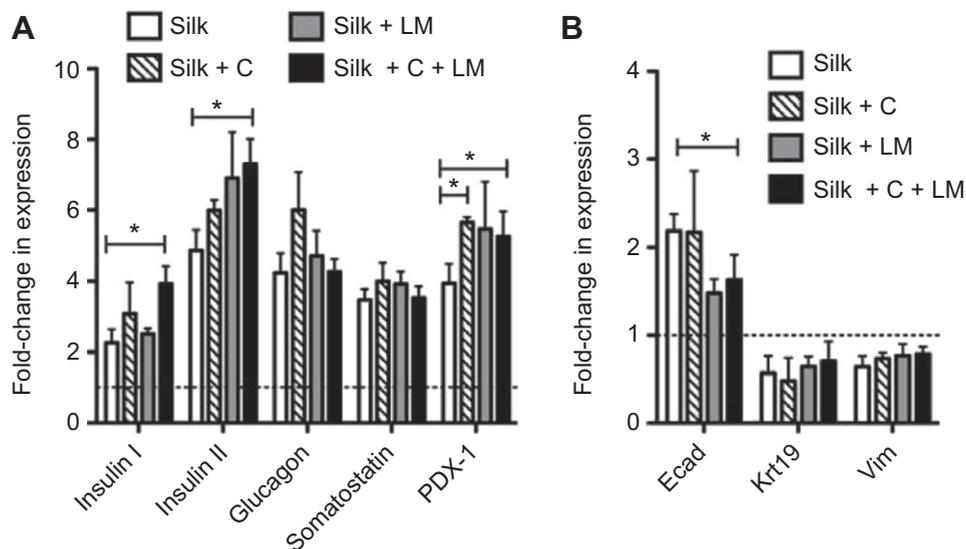

Fig. 3. Relative islet gene expression after a 7 day encapsulation in silk hydrogels with ECM proteins collagen IV (C) and laminin (LM). Fold-change in islet gene expression of functional and regenerative genes (A) and de-differentiation genes, E-cadherin (Ecad), cytokeratin 19 (Krt19), and vimentin (Vim), (B). Relative gene expression determined by the $\Delta\Delta$CT method relative to the GAPDH gene expression and normalized to non-encapsulated islets (dotted line). All samples are given as mean ± SEM, for all conditions $n \geq 4$, $^*p < 0.05$ compared to islets encapsulated in silk.

lymphocyte reaction, silk encapsulated MSCs suppressed spleno-cyte proliferation by 78% after stimulation with anti-CD3/CD28 beads (Fig. 4A) ($p < 0.001$), and by 70% after allo-stimulation (Fig. 4B) ($p < 0.0001$), confirming the immunomodulatory capacity of MSCs within the hydrogel.

3.6. Co-encapsulation of MSCs improves islet function

The synergistic effects from co-encapsulation of ECM proteins and MSCs on islet insulin secretion were evaluated after 7 days. The SI for islets encapsulated in silk increased to 2.3 with the inclusion of MSCs compared to 1.4 for islets in silk alone ($p = 0.06$) (Fig. 5). The SI for islets encapsulated in silk with collagen IV, laminin and MSCs was 4.4, representing a 3.2-fold increase compared to islets in silk alone ($p < 0.01$).

4. Discussion

In this study, silk hydrogels were evaluated as a biomaterial to co-encapsulate ECM proteins and stromal cells to enhance islet function. Silk fibroin was formulated to have vortex-induced gela-tion, with the kinetics of self-assembly controllable by vortex time, assembly temperature, and protein concentration [16]. Vortex-induced silk hydrogels are a promising injectable islet delivery scaffold due to the rapid gelation time and ability to recover from shear-thinning after being injected through a needle [16]. When encapsulated in the silk hydrogel, islets maintained their morphology, viability, and glucose stimulated insulin secretion. After a 7 day in vitro encapsulation, islet shape and the physical integrity of the surrounding capsule were maintained, which has been reported to be critical for metabolic function [20].

In a normal pancreas, islets are surrounded by an ECM capsule composed of collagen I, collagen IV, laminin, and fibronectin that binds to integrins on the islet surface to provide structural support, mediate cell adhesion, and activate intracellular signaling pathways [20,21]. During islet isolation, vasculature and cell-matrix connec-tions are reduced, resulting in suboptimal cell function, and ulti-mately graft failure [10,22–25]. For this reason two ECM proteins (collagen IV and laminin) were added to the silk scaffold to enhance encapsulated islet cell integrin signaling and to increase cell survival and insulin secretion. The addition of collagen IV and laminin did not improve viability, and had modest effects on insulin secretion in response to glucose. Islet insulin secretion was stim-ulated by glucose at diabetic physiological concentrations of basal (2.8 mM) and hyperglycemic (16.7 mM) levels. Encapsulated islets secreted higher concentrations of insulin when subjected to greater glucose levels with stimulation indices greater than one, and similar to previously reported in vitro cultures of islets on ECM-modified surfaces [26] and encapsulated in synthetic biomaterials [27]. At 2 days, islets in silk with collagen IV had the greatest insulin response. However, after a 7 day encapsulation, islets in silk with laminin performed better than islets with collagen IV, in agreement with previously published results [7]. The changes in islet function are likely due to integrin signaling since the addition of ECM proteins did not change the material modulus of the hydrogel as determined by rheology. Surprisingly, islets encapsulated with both laminin and collagen IV had reduced function compared to islets with a single ECM protein, contrary to the synergistic effects observed by Weber et al. [7]. The absence of enhanced synergistic islet function with both ECM proteins may be attributed to the unique properties of the silk amino acid sequence and secondary structure within the hydrogel.

qRT-PCR analysis for islet functional genes confirmed the bene-ficial effects of islet encapsulation in silk hydrogels with ECM proteins. Islets encapsulated in silk had increased expression of all functional genes: insulin I and II, glucagon, somatostatin, and PDX-1 compared to non-encapsulated cells, consistent with previous studies of islets cultured on ECM-modified surfaces and scaffolds [26,28]. The increased gene expression may be attributed to the physical interactions provided by the silk three-dimensional encapsulation, resulting in integrin receptor activation. In the silk hydrogel, islets with both collagen IV and laminin showed a signif-icant increase in β-cell insulin gene expression, but not enhanced insulin protein secretion compared to islets in silk in the absence of ECM proteins (illustrated by Figs. 3A and 2B respectively). Never-theless, the increased islet functional gene expression suggests that the silk hydrogel may be a promising biomaterial for long-term maintenance of islet function.

Cell encapsulation in the silk-based biomaterial preserved the highly differentiated state of islet cells. E-cadherin is an adhesion molecule important for maintaining the balance between insulin secretion and β-cell proliferation [29–31]. Islets in silk had
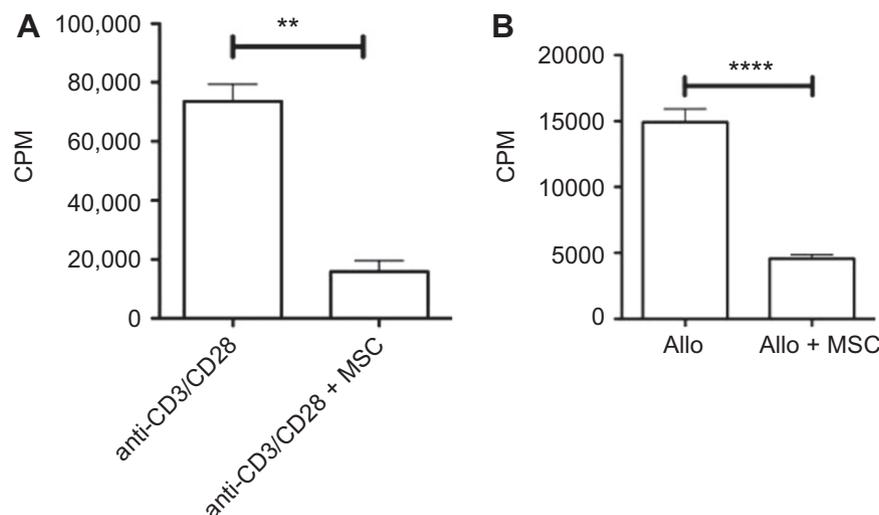
Fig. 4. MSC immunomodulatory ability in silk. Bone marrow derived mouse MSCs encapsulated in silk suppress splenocyte proliferation in response to anti-CD3/CD28 cross-linking (A) or allogeneic antigen stimulation (B) at a 1:1 MSC:splenocyte ratio. The results are expressed as the mean counts per minute (cpm) ± SEM, for all conditions $n \geq 3$, **$p < 0.001$, and ****$p < 0.0001$.
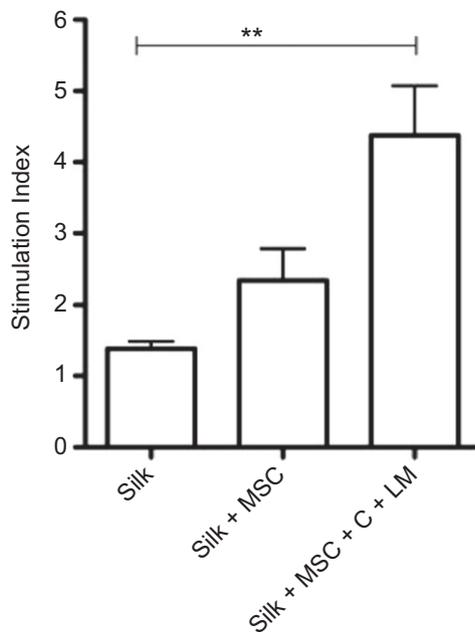
Fig. 5. Islet response to glucose stimulation after a 7 day encapsulation with MSCs and ECM proteins collagen IV (C) and laminin (LM). Islet insulin secretion is given as a stimulation index, which is the ratio of insulin secreted in response to 16.7 mM glucose to insulin secreted in response to 2.5 mM glucose, after 7 days of encapsulation, mean ± SEM, for all conditions $n \geq 4$, $**p < 0.01$, compared to non-encapsulated islets.

increased gene expression levels of E-cadherin, which correlates with optimal metabolic function [32–34]. During islet *ex vivo* processing, islets may dedifferentiate into fibroblast-like cells [35–37] and acquire expression of the ductal and epithelial markers cytokeratin 19 and vimentin [37,38]. Importantly, silk encapsulated islets had decreased expression of both cytokeratin 19 and vimentin as compared to non-encapsulated islets, suggesting that the three-dimensional silk matrix may prevent islet de-differentiation.

The silk scaffold allows for co-delivery and co-localization of secondary stromal cells. Islets co-cultured with secondary cell types, such as fibroblasts and stromal cells have increased function *in vitro*, and greater graft viability and longevity *in vivo* [14,39,40]. In the silk hydrogel, islets that were co-encapsulated with bone marrow derived MSCs had enhanced β-cell response to glucose stimulation compared to islets alone; suggesting the ability of MSCs to affect islet function either through cell–cell contact or the secretion of soluble trophic factors in the silk. Interestingly, islet cell metabolic function was greatest when co-encapsulated with MSCs and ECM proteins in the silk hydrogels. This synergistic effect may be explained by additional trophic factors secreted by MSCs in contact with ECM proteins. Furthermore, silk encapsulated MSCs secrete immunosuppressive soluble factors that may decrease inflammation and immunogenicity as shown by the suppression of splenocyte proliferation in the mixed lymphocyte stimulation assay. Previously, MSCs have been shown to exert immunomodulatory properties on T cells by the secretion of soluble molecules such as: 2,3-dioxygenase, prostaglandin-E2, nitric oxide, and transforming growth factor-β [41,42]. Furthermore, matrix metalloproteinases secreted by MSCs cleave CD25 from T cell surfaces, impeding activation and expansion of alloreactive T cells [14]. Further analysis both *in vitro* and *in vivo* is ongoing in our laboratory to determine the specific humoral factors secreted by MSCs co-encapsulated with islets in the silk hydrogel.

Initial *in vitro* evaluation suggests that silk hydrogels may be a promising platform for islet encapsulation and transplantation;

however, further evaluation *in vivo* is required to ensure that silk is a robust platform for long-term islet engraftment and function. First, the silk hydrogel material properties should be optimized to facilitate physical implantation *in vivo*. Second, the ideal hydrogel degradation rate should be determined for islet encapsulation. It may be beneficial to have an *in vivo* hydrogel that has minimal or a very slow degradation rate. Although our initial observations and previous research suggests silk is non-immunogenic [43], further *in vivo* evaluations in our laboratory are addressing the formation of a fibrous capsule around the implant and the potential host immune response in animal models of T1D.

5. Conclusion

The work presented herein demonstrates the potential utility of silk-based hydrogels as islet encapsulation platforms for transplantation. Silk, despite being used as a biomaterial for centuries, has had minimal investigation as an islet encapsulation material. Our results demonstrate that silk hydrogels provide a permissive 3D environment for encapsulating islets *in vitro,* to maintain islet function and viability. Furthermore, the vortex-induced silk hydrogels allow for the co-encapsulation of extracellular-matrix proteins and secondary stromal cells, that can further enhance islet function. In addition, the versatility of the silk-based hydrogel allows for co-encapsulation of islets with other types of stromal cells, peptides, or proteins, as well as β-cells derived from other sources that may ultimately produce a functional transplantation device to treat T1D.

Acknowledgments

References

[1] Shapiro AMJ, Lakey JRT, Ryan EA, Korbutt GS, Toth E, Warnock GL, et al. Islet transplantation in seven patients with type 1 diabetes mellitus using a glucocorticoid-free immunosuppressive regimen. N Engl J Med 2000;343: 230–8.

[2] Ryan EA, Paty BW, Senior PA, Bigam D, Alfadhli E, Kneteman NM, et al. Five-year follow-up after clinical islet transplantation. Diabetes 2005;54:2060–9.

[3] Stendahl JC, Wang LJ, Chow LW, Kaufman DB, Stupp SI. Growth factor delivery from self-assembling nanofibers to facilitate islet transplantation. Transplantation 2008;86:478–81.

[4] Su J, Hu BH, Lowe WL, Kaufman DB, Messersmith PB. Anti-inflammatory peptide-functionalized hydrogels for insulin-secreting cell encapsulation. Biomaterials 2010;31:308–14.

[5] Beck J, Angus R, Madsen B, Britt D, Vernon B, Nguyen KT. Islet encapsulation: strategies to enhance islet cell functions. Tissue Eng 2007;13:589–99.

[6] Wang YZ, Kim HJ, Vunjak-Novakovic G, Kaplan DL. Stem cell-based tissue engineering with silk biomaterials. Biomaterials 2006;27:6064–82.

[7] Weber LM, Anseth KS. Hydrogel encapsulation environments functionalized with extracellular matrix interactions increase islet insulin secretion. Matrix Biol 2008;27:667–73.

[8] Weber LM, Hayda KN, Anseth KS. Cell-matrix interactions improve beta-cell survival and insulin secretion in three-dimensional culture. Tissue Eng Part A 2008;14:1959–68.

[9] Goto M, Yoshikawa Y, Matsuo K, Shirasu A, Ogawa N, Takahashi H, et al. Optimization of a prominent oxygen-permeable device for pancreatic islets. Transplant Proc 2008;40:411–2.

[10] Ilieva A, Yuan S, Wang RN, Agapitos D, Hill DJ, Rosenberg L. Pancreatic islet cell survival following islet isolation: the role of cellular interactions in the pancreas. J Endocrinol 1999;161:357–64.

[11] Schinkothe T, Bloch W, Schmidt A. In vitro secreting profile of human mesenchymal stem cells. Stem Cells Dev 2008;17:199–205.

[12] Meirelles LdS, Fontes AM, Covas DT, Caplan AI. Mechanisms involved in the therapeutic properties of mesenchymal stem cells. Cytokine Growth Factor Rev 2009;20:419–27.

[13] Boumaza I, Srinivasan S, Witt WT, Feghali-Bostwick C, Dai YF, Garcia-Ocana A, et al. Autologous bone marrow-derived rat mesenchymal stem cells promote PDX-1 and insulin expression in the islets, alter T cell cytokine pattern and preserve regulatory T cells in the periphery and induce sustained normoglycemia. J Autoimmun 2009;32:33–42.

[14] Ding YC, Xu DM, Feng G, Bushell A, Muschel RJ, Wood KJ. Mesenchymal stem cells prevent the rejection of fully allogenic islet grafts by the immunosuppressive activity of matrix metalloproteinase-2 and-9. Diabetes 2009;58:1797–806.

[15] Nauta AJ, Fibbe WE. Immunomodulatory properties of mesenchymal stromal cells. Blood 2007;110:3499–506.

[16] Yucel T, Cebe P, Kaplan DL. Vortex-induced injectable silk fibroin hydrogels. Biophys J 2009;97:2044–50.

[17] Li DS, Yuan YH, Tu HJ, Liang QL, Dai LJ. A protocol for islet isolation from mouse pancreas. Nat Protoc 2009;4:1649–52.

[18] Peister A, Mellad JA, Larson BL, Hall BM, Gibson LF, Prockop DJ. Adult stem cells from bone marrow (MSCs) isolated from different strains of inbred mice vary in surface epitopes, rates of proliferation, and differentiation potential. Blood 2004;103:1662–8.

[19] Livak KJ, Schmittgen TD. Analysis of relative gene expression data using real-time quantitative PCR and the 2(T)(-Delta Delta C) method. Methods 2001;25:402–8.

[20] Stendahl JC, Kaufman DB, Stupp SI. Extracellular matrix in pancreatic islets: relevance to scaffold design and transplantation. Cell Transplant 2009;18:1–12.

[21] Wang RN, Rosenberg L. Maintenance of beta-cell function and survival following islet isolation requires re-establishment of the islet-matrix relationship. J Endocrinol 1999;163:181–90.

[22] Vogel WF. Collagen-receptor signaling in health and disease. Eur J Dermatol 2001;11:506–14.

[23] Kaido T, Yebra M, Cirulli V, Montgomery AM. Regulation of human beta-cell adhesion, motility, and insulin secretion by collagen IV and its receptor alpha(1)beta(1). J Biol Chem 2004;279:53762–9.

[24] Labriola L, Montor WR, Krogh K, Lojudice FH, Genzini T, Goldberg AC, et al. Beneficial effects of prolactin and laminin on human pancreatic islet-cell cultures. Mol Cell Endocrinol 2007;263:120–33.

[25] Brendel MD, Kong SS, Alejandro R, Mintz DH. Improved functional survival of human islets of langerhans in 3-dimensional matrix culture. Cell Transplant 1994;3:427–35.

[26] Daoud J, Petropavlovskaia M, Rosenberg L, Tabrizian M. The effect of extracellular matrix components on the preservation of human islet function in vitro. Biomaterials 2010;31:1676–82.

[27] Chow LW, Wang LJ, Kaufman DB, Stupp SI. Self-assembling nanostructures to deliver angiogenic factors to pancreatic islets. Biomaterials 2010;31:6154–61.

[28] Daoud JT, Petropavlovskaia MS, Patapas JM, Degrandpre CE, DiRaddo RW, Rosenberg L, et al. Long-term in vitro human pancreatic islet culture using three-dimensional microfabricated scaffolds. Biomaterials 2011;32:1536–42.

[29] Carvell MJ, Marsh PJ, Persaud SJ, Jones PM. E-cadherin interactions regulate beta-cell proliferation in islet-like structures. Cell Physiol Biochem 2007;20:617–26.

[30] Hauge-Evans AC, Squires PE, Persaud SJ, Jones PM. Pancreatic beta-cell-to-beta-cell interactions are required for integrated responses to nutrient stimuli - enhanced Ca2+ and insulin secretory responses of MIN6 pseudoislets. Diabetes 1999;48:1402–8.

[31] Yamagata K, Nammo T, Moriwaki M, Ihara A, Iizuka K, Yang Q, et al. Over-expression of dominant-negative mutant hepatocyte nuclear factor-1 alpha in pancreatic beta-cells causes abnormal islet architecture with decreased expression of E-cadherin, reduced beta-cell proliferation, and diabetes. Diabetes 2002;51:114–23.

[32] Schmied BM, Ulrich A, Matsuzaki H, Ding XZ, Ricordi C, Weide L, et al. Transdifferentiation of human islet cells in a long-term culture. Pancreas 2001;23:157–71.

[33] Schmied BM, Ulrich A, Matsuzaki H, Ding XZ, Ricordi C, Moyer MP, et al. Maintenance of human islets in long term culture. Differentiation 2000;66:173–80.

[34] Beattie GM, Montgomery AMP, Lopez AD, Hao E, Perez B, Just ML, et al. A novel approach to increase human islet cell mass while preserving beta-cell function. Diabetes 2002;51:3435–9.

[35] Weinberg N, Ouziel-Yahalom L, Knoller S, Efrat S, Dor Y. Lineage tracing evidence for in vitro dedifferentiation but rare proliferation of mouse pancreatic beta-cells. Diabetes 2007;56:1299–304.

[36] Ouziel-Yahalom L, Zalzman M, Anker-Kitai L, Knoller S, Bar Y, Glandt M, et al. Expansion and redifferentiation of adult human pancreatic islet cells. Biochem Biophys Res Commun 2006;341:291–8.

[37] Gershengorn MC, Hardikar AA, Wei CJ, Geras-Raaka E, Marcus-Samuels B, Raaka BM. Epithelial-to-mesenchymal transition generates proliferative human islet precursor cells. Science 2004;306:2261–4.

[38] Joglekar MV, Joglekar VM, Joglekar SV, Hardikar AA. Human fetal pancreatic insulin-producing cells proliferate in vitro. J Endocrinol 2009;201:27–36.

[39] Park K-S, Kim Y-S, Kim J-H, Choi B, Kim S-H, Tan AH-K, et al. Trophic molecules derived from human mesenchymal stem cells enhance survival, function, and angiogenesis of isolated islets after transplantation. Transplant 2010;89:509–17.

[40] Jalili RB, Rezakhanlou AM, Hosseini-Tabatabaei A, Ao Z, Warnock GL, Ghahary A. Fibroblast populated collagen matrix promotes islet survival and reduces the number of islets required for diabetes reversal. J Cell Physiol. 2011;226:1813–9.

[41] Abdi R, Fiorina P, Adra CN, Atkinson M, Sayegh MH. Immunomodulation by mesenchymal stem cells - a potential therapeutic strategy for type 1 diabetes. Diabetes 2008;57:1759–67.

[42] Yagi H, Soto-Gutierrez A, Parekkadan B, Kitagawa Y, Tompkins RG, Kobayashi N, et al. Mesenchymal stem cells: mechanisms of immunomodulation and homing. Cell Transplant 2010;19:667–79.

[43] Altman GH, Diaz F, Jakuba C, Calabro T, Horan RL, Chen JS, et al. Silk-based biomaterials. Biomaterials 2003;24:401–16.